

# Electron correlations in $\text{Co}_2\text{Mn}_{1-x}\text{Fe}_x\text{Si}$ Heusler compounds.

Stanislav Chadov, Gerhard H. Fecher, and Claudia Felser

E-mail: [chadov@uni-mainz.de](mailto:chadov@uni-mainz.de)

Institut für Anorganische und Analytische Chemie, Johannes Gutenberg -  
Universität Mainz, 55099 Mainz, Germany

Jan Minár, Jürgen Braun, and Hubert Ebert

Dept. Chemie und Biochemie, Physikalische Chemie, Universität München,  
Butenandtstr. 5-13, 81377 München, Germany

## Abstract.

This study presents the effect of local electronic correlations on the Heusler compounds  $\text{Co}_2\text{Mn}_{1-x}\text{Fe}_x\text{Si}$  as a function of the concentration  $x$ . The analysis has been performed by means of first-principles band-structure calculations based on the local approximation to spin-density functional theory (LSDA). Correlation effects are treated in terms of the Dynamical Mean-Field Theory (DMFT) and the LSDA+U approach. The formalism is implemented within the Korringa-Kohn-Rostoker (KKR) Green's function method.

In good agreement with the available experimental data the magnetic and spectroscopic properties of the compound are explained in terms of strong electronic correlations. In addition the correlation effects have been analysed separately with respect to their static or dynamical origin. To achieve a quantitative description of the electronic structure of  $\text{Co}_2\text{Mn}_{1-x}\text{Fe}_x\text{Si}$  both static and dynamic correlations must be treated on equal footing.

PACS numbers: 71.27.+a, 7.20.Be, 7.15.Mb

*Keywords:* Heusler compounds, half-metallic, correlations, KKR, DMFT, LSDA, LSDA+U

Submitted to: *J. Phys. D: Appl. Phys.*

## 1. Introduction

One of the most interesting class of materials for magneto-electronic applications is found in the family of  $\text{Co}_2\text{YZ}$  half-metallic Heusler ferromagnets [1, 2]. Special technological attention has been paid to the  $\text{Co}_2\text{MnSi}$  compound because of a predicted large minority band gap (0.4 eV) and a very high Curie temperature (985 K) among the variety of Heusler compounds [3–6]. However, an even more interesting material,  $\text{Co}_2\text{FeSi}$ , was found in recent investigations [7–9] exhibiting a Curie temperature of about 1100 K and a very high magnetic moment of  $6 \mu_B$  in the primitive cell. Later on it was shown that the complete substitutional series  $\text{Co}_2\text{Mn}_{1-x}\text{Fe}_x\text{Si}$  crystallises in the Heusler type  $L2_1$  structure with a high degree of structural order [10]. Also confirmed was a Slater-Pauling behaviour (see [5, 11, 12]) of the magnetic moment ranging linearly from  $5 \mu_B$  to  $6 \mu_B$  with increasing Fe concentration  $x$ .

A detailed understanding of the electronic and magnetic structure of half-metallic ferromagnets, their surfaces and corresponding nanostructures is directly connected with an improved theoretical description based on first-principle methods. From previous studies [13, 14] it follows that quantitative calculations of the electronic structure of  $\text{Co}_2\text{Mn}_{1-x}\text{Fe}_x\text{Si}$  compounds require a correct incorporation of local correlation effects. For example, a former study [13] applying the LSDA+U method [15, 16] was able to reproduce the experimental band gap as well as the correct values of the magnetic moments when using reasonable values for the parameters  $U$  and  $J$  and when also including the appropriate double-counting corrections. Similar results [10] were obtained by applying the GGA approach which also takes into account correlations beyond the LSDA-scheme. In the present analysis electronic correlation effects have been treated in the framework of the Dynamical Mean-Field Theory [17], which quantitatively takes into account dynamical correlation effects, in particular spin-flip processes induced by fluctuations. In combination with the LSDA (LSDA+DMFT) this formalism provides a very reliable approach to deal with a wide range of static and spectroscopic properties of  $3d$  transition metals. These are, for example, total energies, magnetic moments, magneto-optical properties and photoemission intensities [18–23].

The most serious complication when combining LSDA with DMFT arises from the double-counting problem. As it has been indicated by numerous DMFT studies, the static many-body effects which are typically over counted in LSDA+DMFT calculations are relatively small in  $3d$  transition metals. Therefore, the established procedure concerning the description of spectroscopic properties is to neglect the static part of the self-energy, setting this term to zero at the Fermi level [18, 19, 24]. However, it was recently shown [22], that this approximation is not sufficient for an accurate description of angle-resolved photoemission spectra of Ni. In this case an additional static polarisation term, which is spin- and orbital-dependent had to be included in the calculations. Later it was demonstrated [23] that using LSDA+U as a static limit for DMFT leads to an improved description of the orbital and spin magnetic moments in a wide range of the  $3d$  transition metal compounds.

Another recent investigation on  $\text{Co}_2\text{MnSi}$  [25], which is based on the assumption that static correlations are already accounted by the LSDA, thus considering only dynamical contributions in the self-energy, supports the existence of the so-called non-quasiparticle states [26]. However, the insufficient treatment of static correlations resulted in a wrong position of the Fermi level, which in the case of  $\text{Co}_2\text{MnSi}$  [13, 14] must be situated closer to the lower edge of the band gap. Similar findings can be obtained from former investigations [27] based on plain LSDA calculations. Therefore, the position of the Fermi level with respect to the band gap is controlled more by the static rather than by the dynamic correlations.

In the present work, both static and dynamic correlations are taken into account simultaneously by combining them as it was done in [23].

## 2. Computational details

The calculations were performed within the relativistic full-potential Korringa-Kohn-Rostoker Green's function (SPR-KKR) method [28]. The DMFT-solver consists in the relativistic version of the so-called Spin Polarised T-Matrix Plus Fluctuation Exchange (SPTF) approximation [24, 29] using the real-energy axis formalism [30]. According to this scheme the local Green's function is obtained by the corresponding site projection of the full KKR Green's function. The local Green's function is needed to obtain the bath Green's function for the Anderson impurity model via the saddle-point equation. The bath Green's function is used as input for the SPTF DMFT-scheme to calculate the local self-energy. The latter appears as an additional energy-dependent potential in the radial Dirac equation which is solved in order to calculate the new full KKR Green's function. This procedure is repeated until self-consistency in both the self-energy and the charge density is achieved. This scheme has been already successfully applied for the description of magneto-optical [31] and magnetic [23] properties of  $3d$  transition metals. Also photoemission intensities [32], including the corresponding matrix element effects, were obtained in quantitative agreement with the experiment.

The static double-counting is treated in the form of the so-called "around atomic limit" (AAL) [16] which is appropriate in the case of integer orbital occupation numbers and therefore corresponds to the half-metals. Although, different mechanisms exist that lead to half-metallicity, in the case of locally correlated half-metals the AAL tends to increase the spin magnetic moment, which is often underestimated in plain LSDA calculations [7]. The self-energy within the DMFT is parameterised by the averaged screened Coulomb interaction  $U$  and the Hund exchange interaction  $J$ . For the latter the screening is usually not crucial; the value of  $J$  can be calculated directly from LSDA and is approximately equal to 0.9 eV for all  $3d$  elements. This value has been adopted for all calculations presented here. Different methods in calculating the screened Coulomb interaction  $U$  for the metallic  $3d$  transition metal systems lead to  $U$ -values in the range between 2-3 eV. In our analysis we keep the  $U$  parameter fixed at 3 eV which is often used for  $3d$  transition metals.

The random substitutional order of the Mn-Fe compounds is treated within the so-called Coherent Potential Approximation (CPA). Since the CPA approach can be formulated in the multiple scattering formalism [33,34] it has a rather straightforward implementation within the KKR method [35]. As it follows from the experiment the lattice constant does not change substantially its value within the whole range of concentrations  $x$ . The lattice parameter was fixed to 5.658 Å in the present study.

Concerning the calculation of the ground state properties few additional details have to be mentioned at this stage. In particular we stress the importance of the full potential treatment, which often leads to some improvements in the description of the band gap already in plain LSDA calculations. On the other hand, one has to increase the  $l$ -value for the expansion in spherical harmonics. This typically improves the calculated value for the band gap and for the magnetic moments. In our case we used  $l_{\max} = 3$  ( $f$  electrons).

The 8 keV valence-band photoemission spectra (VB-XPS) were calculated using the formalism derived by Ebert and Schwitalla [36], which is based on the so-called one-step model of photoemission. In addition, a quantitative treatment of core-hole effects on the valence states turned out to be of crucial importance for a correct description of hard X-ray VB-XPS. Here, the presence of the core-hole was explicitly accounted for when calculating the initial state. Here, we used the static so-called  $Z + 1$  approach [37]. This means that the electronic structure has to be calculated self-consistently with a core state of the excited atom (here  $1s$  of Mn) being unoccupied. The missing charge is added to the valence band.

Another important aspect which one has to consider in calculations of hard X-ray photoemission is the correct treatment of the X-ray cross-section as a function of the photon energy. It follows from the calculations (see [14]) that the cross-sections for  $p$  and  $d$  electrons are nearly the same for kinetic energies of 3-4 keV. However, at 8 keV their ratios are completely different, in particular the  $d$  cross-section becomes much smaller. In the present work these effects are taken into account implicitly within the one-step formalism. On the other hand the uncertainty in the calculation of the final state increases with increasing photon energy, because of an increasing number of oscillations in the final state radial wave functions. Therefore, one needs to account for a much larger number of points on the radial mesh in order to reproduce these variations correctly.

In order to account for the experimental resolution, the calculated spectra were convoluted by a Gaussian with FWHM = 0.025 eV. For a direct comparison, the background intensity was subtracted from the experimental data using the Shirley procedure [38].

### 3. Results and discussion

#### *Ground-state properties*

As it was mentioned above, a quantitative treatment of static correlations is important for a reliable description of the minority band gap as well as of the magnetic moments in correlated half-metals. More details can be found in preceding publications [7]. Our calculations show a noticeable increase of the magnetic moments in analogy to the Slater-Pauling curve within the whole range of concentrations (see figure 1). By construction, the dynamical part of the local self-energy  $\Sigma$  in the vicinity of the Fermi level describes Fermi liquid behaviour, i.e.  $\text{Re}\Sigma(\epsilon) \sim -(\epsilon - \epsilon_F)$ ,  $\text{Im}\Sigma(\epsilon) \sim -(\epsilon - \epsilon_F)^2$ . Therefore, we do not expect a substantial change for the integral quantities by accounting only for dynamical correlations. Indeed, as it follows from figure 1, the magnetic moments calculated with LSDA+DMFT are only slightly reduced comparing to those obtained from LSDA+U. This small decrease may be attributed to the spin-flip events induced by the dynamical fluctuations leading to the so-called non-quasiparticle states absent in the LSDA treatment [25]. At the same time the effect of static correlations on the magnetic moment is more pronounced for the Fe-rich limit of the concentration  $x$ .

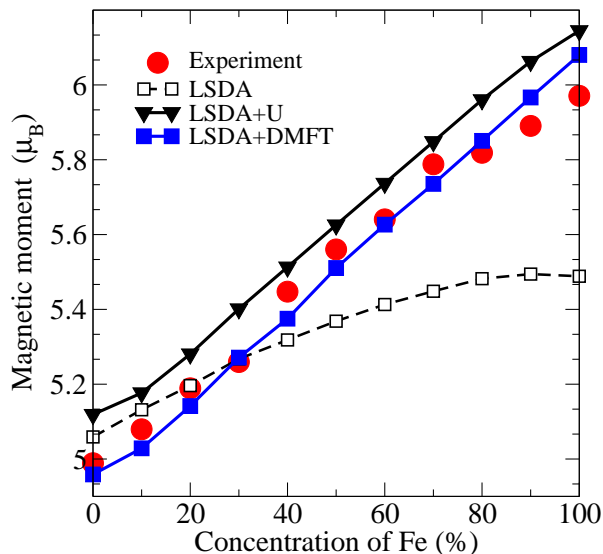


**Figure 1.** Comparison of the total magnetic moments for  $\text{Co}_2\text{Mn}_x\text{Fe}_{1-x}\text{Si}$  compounds calculated within LSDA (black dashed line, opened squares), LSDA+U (black triangles) and LSDA+DMFT (blue squares) with the results of the SQUID magnetic measurements (red circles) [39].

The dynamical correlations appear to be more significant for the spectroscopic properties. As it follows from figure 2, the LSDA+U shifts the  $d$  states away from the Fermi level creating a band gap in the minority-spin channel. At the same time adding the dynamical correlations tend to narrow the bandwidth by shifting the states back to the Fermi level, however without influencing the band gap itself. One also can observe

a substantial broadening of the DOS within the range between  $-2$  to  $-8$  eV, which is due to the imaginary part of the energy-dependent self-energy.

It follows from the DOS curves, that the enhancement of the magnetic moment with the increase of the Fe concentration (see figure 2) is connected to the corresponding shift of the Fermi energy across the band-gap. In both limiting cases one observes the non-vanishing minority-spin states at the Fermi level. This indicates that both  $\text{Co}_2\text{MnSi}$  and  $\text{Co}_2\text{FeSi}$  may not represent fully spin polarised ferromagnets in contrast to the compounds with intermediate Fe concentrations.

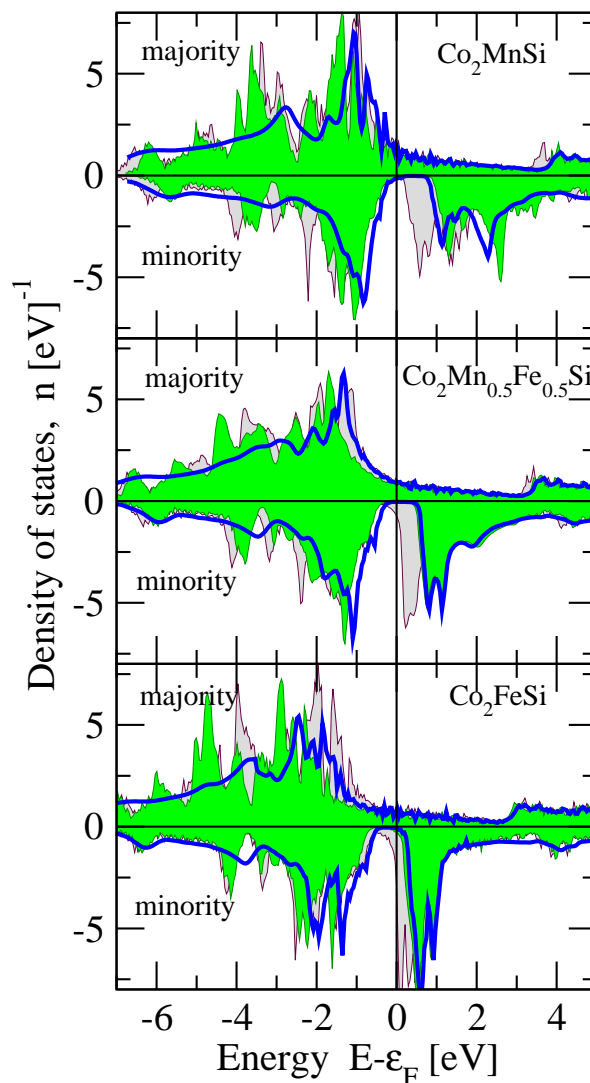


**Figure 2.** The total spin-resolved DOS curves for  $\text{Co}_2\text{MnSi}$ ,  $\text{Co}_2\text{Mn}_{0.5}\text{Fe}_{0.5}\text{Si}$  and  $\text{Co}_2\text{FeSi}$  calculated within LSDA (light/grey filled area), LSDA+U (dark/green filled area) and LSDA+DMFT (blue line).

*Photoemission*

It was mentioned above, that an important issue is to account for the electron interaction with holes created in the photoemission process. The hole life-time increases when approaching the core energies. Therefore, the core holes itself have the longest life times and in consequence the most pronounced influence on the photoemission spectra. According to the experimentally available core energies the 8 keV photon beam used in the measurements corresponds to the excitation of the  $1s$  states of Mn. This assumption agrees well with the results obtained in a preceding investigation [14]. Indeed, comparing the experimental photoemission data to the calculated DOS one notices that the latter must be scaled on the energy axis by a factor of about 1.1 in case of  $\text{Co}_2\text{MnSi}$ . However, in the case of  $\text{Co}_2\text{FeSi}$  (with no manganese) the  $-10$  eV  $s$ -peak is already in good agreement with the experiment. In the present paper we account for this effect explicitly by introducing in the self-consistent calculation for  $\text{Co}_2\text{MnSi}$  a core hole in the Mn  $1s$  level. The corresponding change in the DOS is shown in figure 3. Since the account of correlation effects in the actual photoemission calculations is essentially based on a ground-state information, the core hole is accounted for just by simply scaling the final result by a factor of 1.1 times the concentration of Mn along the energy axis.

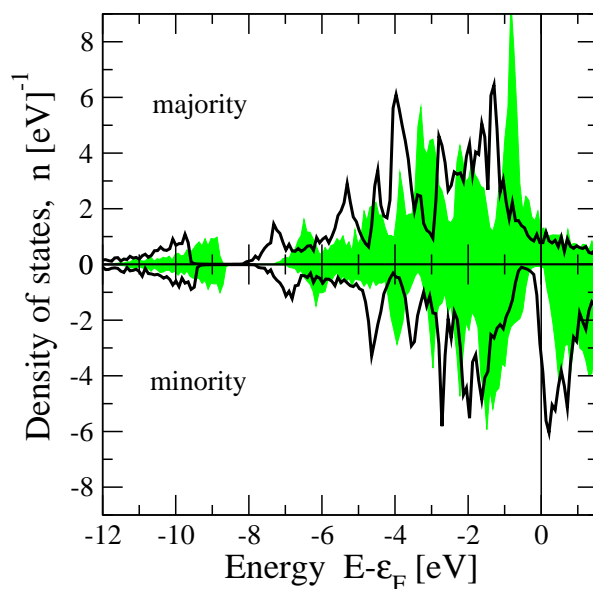


**Figure 3.** Comparison of the total spin-resolved (LSDA) DOS curves for  $\text{Co}_2\text{MnSi}$  in case of the hole created in  $1s$  core level of Mn (black line) and without (green filled area).

The influence of correlation effects in VB-XPS is illustrated in Fig. 4. It follows, that the consideration of static correlations (LSDA+U) substantially improves the plain LSDA result in the range above  $-5$  eV, reproducing the  $-1$  eV and  $-4$  eV peaks, which are shifted comparing to plain LSDA by about  $0.5$  eV to higher binding energies. Even more, tiny features such as the local minima at  $-1.5$  eV,  $-2.5$  eV and the peak splittings

are well reproduced. Not only the peak positions but also the intensities above  $-5$  eV were improved in comparison to the experiment, while only the  $-4$  eV peak appears to be much too intense. Various attempts to treat the final states more accurately did not change this situation substantially. Therefore, it is concluded that the origin of this discrepancy is found in a band-structure effect caused by the Si  $p$  states and by the  $d$  states of Mn and Co. Indeed, the corresponding total DOS spectra (see figure 2) show the most intensive peak at about  $-3$  eV binding energy, which is formed by the corresponding  $p$  and  $d$  states. As discussed above one has to scale the DOS energy axis by a factor of 1.1 in order to compare with the VB-XPS. At high photon energies the cross-section of the  $p$  states is larger than for the  $d$  states, however the later ones have larger spectral weight. Therefore, the contributions of  $p$  and  $d$  states are comparable.

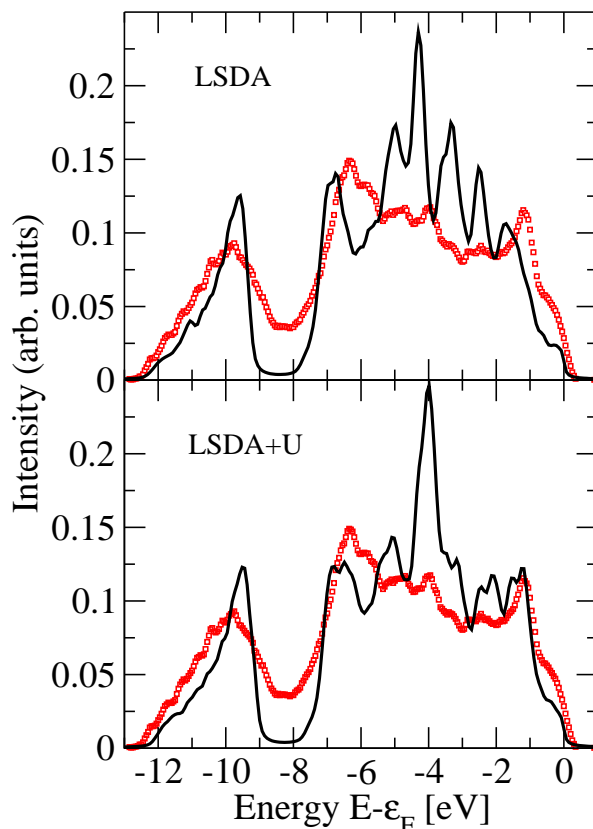


**Figure 4.** Comparison of the theoretical (solid lines) 8 keV VB-XPS spectra for  $\text{Co}_2\text{MnSi}$  calculated within plain LSDA and LSDA+U to the experiment (red squares) [14]. The area under each curve is normalised to unity and  $1s$  core-hole effects of Mn are included.

The result of the complete correlation schemes illustrated in the top panel of figure 5. In conclusion, it follows that inclusion of DMFT makes some important improvements for the VB-XPS spectra by correcting the amplitudes and the positions of the  $-1$  eV and  $-10$  eV peaks. Also the intermediate area between  $-10$  and  $-6$  eV binding energy shows a very close agreement with experiment. The position of the  $-6$  eV



peak formed by  $p$  states of Si is still not perfectly reproduced, however it is moved in the proper direction compared to LSDA+U result. The pronounced spectral feature observable at  $-4$  eV is substantially reduced in intensity, but it is still overestimated by theory. The position is slightly shifted towards the Fermi level induced by the real part of the energy-dependent self-energy. The corresponding shift of the DOS is seen in figure 2. The energy regime ranging from  $-8.5$  to  $-4.5$  eV binding energy corresponds to the maximal amplitude of the imaginary component of the self-energy. From figure 5, it follows that this causes some Lorentzian over-broadening of the features at  $-4.5$  eV for all calculated concentrations. On the other hand it perfectly describes the so-called Heusler gap at about  $-8.5$  eV. Thus, it is concluded that a non-zero intensity in the Heusler gap is mostly determined by the electron ground states existing in this region, rather than by background effects.

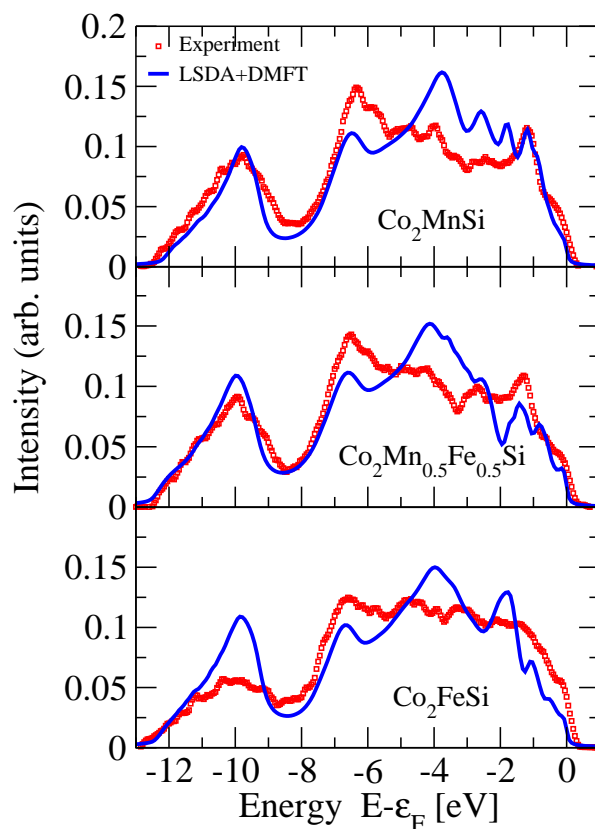


**Figure 5.** The 8 keV VB-XPS spectra for  $\text{Co}_2\text{MnSi}$ ,  $\text{Co}_2\text{Mn}_{0.5}\text{Fe}_{0.5}\text{Si}$  and  $\text{Co}_2\text{FeSi}$  calculated within LSDA+DMFT (solid line) compared to the experiment (squares) [14]. The area under each curve is normalised to unity and  $1s$  core-hole effects of Mn are included.

#### 4. Summary

From the detailed analysis it follows that  $\text{Co}_2\text{Mn}_{1-x}\text{Fe}_x\text{Si}$  is a very pronounced locally correlated material for which the plain LSDA calculations are insufficient to describe

their electronic and magnetic properties correctly. The values of the magnetic moments and the details of the minority band gap are mostly determined by static correlations. In particular, this influence becomes more significant for the magnetic moments with increasing Fe concentration. A satisfactory description of this effect can be given on the basis of the LSDA+U approach within the AAL type of double-counting.

It turned out, that it is not sufficient to explain all spectral properties accounting for static correlations only. Peak positions and intensities are significantly improved due to the incorporation of dynamical correlations. These correlations can be described quantitatively by the LSDA+DMFT approach.

Obviously, the improvement is not completely perfect and agreement with experiment gets worse with increasing Fe concentration. One reason may be found in the perturbative nature of the used DMFT-solver that affects the ground-state description. However, this is difficult to verify, since more accurate solvers are much more time-consuming and restricted to only very small systems. In principle, the DMFT itself becomes exact only in the limit of infinite coordination numbers [17]. This implies that non-local correlations may also play a role [40]. The uncertainty of the double-counting and values of  $U$  and  $J$  has to be considered, too. Another source of errors is the insufficient description of the excited properties, in particular the uncertainty in dealing with the final states. On the other hand, a very important excitation effect, namely the influence of the core holes was recognised, quantified and taken into account in the present work.

Finally, it is emphasised that the LSDA+DMFT scheme used in this work has significantly improved the description of the magnetism and VB-XPS in the presented series of Heusler compounds with  $L2_1$  structure. This result is in accordance with former studies on  $3d$  transition metals.

## Acknowledgments

The authors like to thank K. Kobayashi, E. Ikenaga, J.-J. Kim, and S. Ueda for support with the photoemission experiments at Spring-8 (Japan). The HAXPES measurements were performed under the approval of NIMS Beamline Station (Proposal Nos. 2007A4903, 2007B4907) and at BL47XU of Spring-8 (Japan) under the approval of JASRI (Proposal Nos. 2006A1476, 2008A0017). The authors gratefully acknowledge financial support by the Deutsche Forschungsgemeinschaft DFG (Research Unit FOR 559, Project P 7).

## References

- [1] J Kübler, A R Williams, and C B Sommers. *Phys. Rev. B*, 28:1745, 1983.
- [2] C Felser, G H Fecher, and B Balke. *Angew. Chem. Int. Ed.*, 46:668, 2007.
- [3] S Fuji, S Sugimura, S Ishida, and S Asano. *J. Phys. Cond. Matt.*, 2:8583, 1990.
- [4] P J Brown, K-U Normann, P J Webster, and K R A Ziebeck. *J. Phys. Cond. Matt.*, 12:1827, 2000.
- [5] G H Fecher, H C Kandpal, S Wurmehl, C Felser, and G Schönhense. *J. Appl. Phys.*, 99:08J106, 2006.
- [6] J Kübler, G H Fecher, and C Felser. *Phys. Rev. B*, 76:024414, 2007.
- [7] S Wurmehl, G H Fecher, H C Kandpal, V Ksenofontov, C Felser, and H-J Lin. *Phys. Rev. B*, 72:184434, 2005.
- [8] S Wurmehl, G H Fecher, H C Kandpal, V Ksenofontov, C Felser, and H-J Lin. *Appl. Phys. Lett.*, 88:032503, 2006.
- [9] H C Kandpal, G H Fecher, and C Felser. *Phys. Rev. B*, 73:094422, 2006.
- [10] B Balke, G H Fecher, H C Kandpal, C Felser, K Kobayashi, E Ikenaga, J-J Kim, and S Ueda. *Phys. Rev. B*, 74:104405, 2006.
- [11] J Kübler. *Theory of Itinerant Electron Magnetism*. Clarendon Press, Oxford, 2000.
- [12] I Galanakis, P H Dederichs, and N Papanikolaou. *Phys. Rev. B*, 66:174429, 2002.
- [13] H C Kandpal, G H Fecher, C Felser, and G Schönhense. *Phys. Rev. B*, 73:094422, 2006.
- [14] G H Fecher, B Balke, S Ouardi, C Felser, G Schönhense, E Ikenaga, J Kim, S Ueda, and K Kobayashi. *J. Phys. D: Appl. Phys.*, 40:1576, 2007.
- [15] V I Anisimov, J Zaanen, and O K Andersen. *Phys. Rev. B*, 44:943, 1991.
- [16] M T Czyzyk and G A Sawatzky. *Phys. Rev. B*, 49:14211, 1994.
- [17] G Kotliar, S Y Savrasov, K Haule, V S Oudovenko, O Parcolett, and C A Marianetti. *Rev. Mod. Phys.*, 78:865, 2006.
- [18] A I Lichtenstein, M I Katsnelson, and G Kotliar. *Phys. Rev. Lett.*, 87:067205, 2001.
- [19] A Grechnev, I Di Marco, M I Katsnelson, A I Lichtenstein, J Wills, and O Eriksson. *cond-mat*, page 0610621, 2006.
- [20] A Perlov, S Chadov, and H Ebert. *Phys. Rev. B*, 68:245112, 2003.
- [21] J Minár, H Ebert, C de Nadaï, N B Brookes, F Venturini, G Ghiringhelli, L Chioncel, A I Lichtenstein, and M I Katsnelson. *Phys. Rev. Lett.*, 95:166401, 2005.
- [22] J Braun, J Minár, H Ebert, M I Katsnelson, and A I Lichtenstein. *Phys. Rev. Lett.*, 97:227601, 2006.
- [23] S Chadov, J Minár, M I Katsnelson, H Ebert, D Ködderitzsch, and A I Lichtenstein. *Europhys. Lett.*, 82:37001, 2008.
- [24] M I Katsnelson and A Lichtenstein. *Europ. Phys. J. B*, 30:9, 2002.
- [25] L Chioncel, Y Sakuraba, E Arrigoni, M I Katsnelson, M Oogane, Y Ando, T Miyazaki, E Burzoa, and A I Lichtenstein. *Phys. Rev. Lett.*, 100:086402, 2008.
- [26] V Yu Irkin, M I Katsnelson, and A I Lichtenstein. *J. Phys. Cond. Matt.*, 19:315201, 2007.
- [27] S Ishida, S Fuji, S Kashiwagi, and S Asano. *J. Phys. Soc. Jap.*, 64:2152, 1995.
- [28] J Minár, L Chioncel, A Perlov, H Ebert, M I Katsnelson, and A I Lichtenstein. *Phys. Rev. B*, 72:45125, 2005.
- [29] L V Pourovskii, M I Katsnelson, and A I Lichtenstein. *Phys. Rev. B*, 72:115106, 2005.
- [30] V Drchal, V Janiš, and J Kudrnovsky. *Physica B*, 312-313:519, 2002.
- [31] S Chadov, J Minár, H Ebert, A Perlov, L Chioncel, M I Katsnelson, and A I Lichtenstein. *Phys. Rev. B*, 74:140411(R), 2006.
- [32] J Minár, S Chadov, H Ebert, L Chioncel, A Lichtenstein, C de Nadaï, and N B Brookes. *Nuc. Inst. and Met. in Phys. Res. A*, 574:151, 2005.
- [33] B Gyorffy. *Phys. Rev. B*, 5:2382, 1972.
- [34] W H Butler. *Phys. Rev. B*, 31:3260, 1985.

- [35] H Ebert and M Battocletti. *Solid State Comm.*, 98:785, 1996.
- [36] H Ebert and J Schwitalla. *Phys. Rev. B*, 55:3100, 1997.
- [37] M Alouani. *Phys. Rev. B*, 49:16038, 1994.
- [38] D A Shirley. *Phys. Rev. B*, 5:4709, 1972.
- [39] B Balke, G H Fecher, H C Kandpal, and C Felser. *Phys. Rev. B*, 74:104405, 2006.
- [40] J Schäfer, M Hoinkis, E Rotenberg, P Blaha, and R Claessen. *Phys. Rev. B*, 72:155115, 2005.